Bone Marrow Adiposity and Fragility Fractures in Postmenopausal Women: The ADIMOS Case-Control Study

Julien Paccou, Sammy Badr, Daniela Lombardo, Huda Khizindar, Valérie Deken, Stefan Ruschke, Dimitrios C Karampinos, Anne Cotten, Bernard Cortet

The Journal of Clinical Endocrinology & Metabolism, 2023, **00**, 1–11
https://doi.org/10.1210/clinem/dgad195
Advance access publication 5 April 2023
Clinical Research Article

Bone Marrow Adiposity and Fragility Fractures in Postmenopausal Women: The ADIMOS Case-Control Study

Julien Paccou,[1] Sammy Badr,[2] Daniela Lombardo,[1] Huda Khizindar,[2] Valérie Deken,[3] Stefan Ruschke,[4] Dimitrios C. Karampinos,[4] Anne Cotten,[2] and Bernard Cortet[1]

[1]Department of Rheumatology, University Lille, CHU Lille, MABlab ULR 4490, F-59000 Lille, France
[2]Department of Radiology and Musculoskeletal Imaging, University Lille, CHU Lille, MABlab ULR 4490, F-59000 Lille, France
[3]METRICS: Évaluation des technologies de santé et des pratiques médicales, University Lille, CHU Lille, ULR 2694, F-59000 Lille, France
[4]Department of Diagnostic and Interventional Radiology, Klinikum rechts der Isar, School of Medicine, Technical University of Munich, 81675 Munich, Germany

Correspondence: Julien Paccou, MD, PhD, Department of Rheumatology, Lille University Hospital, Rue Emile Laine, F-59000 Lille, France. Email: julien.paccou@chru-lille.fr.

Abstract

Context: Noninvasive assessment of proton density fat fraction (PDFF) by magnetic resonance imaging (MRI) may improve the prediction of fractures.

Objective: This work aimed to determine if an association exists between PDFF and fractures.

Methods: A case-control study was conducted at Lille University Hospital, Lille, France, with 2 groups of postmenopausal women: one with recent osteoporotic fractures, and the other with no fractures. Lumbar spine and proximal femur (femoral head, neck, and diaphysis) PDFF were determined using chemical shift-based water-fat separation MRI (WFI) and dual-energy x-ray absorptiometry scans of the lumbar spine and hip. Our primary objective was to determine the relationship between lumbar spine PDFF and osteoporotic fractures in postmenopausal women. Analysis of covariance was used to compare PDFF measurements between patient cases (overall and according to the type of fracture) and controls, after adjusting for age, Charlson comorbidity index (CCI) and BMD.

Results: In 199 participants, controls (n = 99) were significantly younger ($P < .001$) and had significantly higher BMD ($P < 0.001$ for all sites) than patient cases (n = 100). A total of 52 women with clinical vertebral fractures and 48 with nonvertebral fractures were included. When PDFFs in patient cases and controls were compared, after adjustment on age, CCI, and BMD, no statistically significant differences between the groups were found at the lumbar spine or proximal femur. When PDFFs in participants with clinical vertebral fractures (n = 52) and controls were compared, femoral neck PDFF and femoral diaphysis PDFF were detected to be lower in participants with clinical vertebral fractures than in controls (adjusted mean [SE] 79.3% [1.2] vs 83.0% [0.8]; $P = 0.020$, and 77.7% [1.4] vs 81.6% [0.9]; $P = 0.029$, respectively).

Conclusion: No difference in lumbar spine PDFF was found between those with osteoporotic fractures and controls. However, imaging-based proximal femur PDFF may discriminate between postmenopausal women with and without clinical vertebral fractures, independently of age, CCI, and BMD.

Key Words: osteoporosis, fracture, bone marrow adipose tissue, bone mineral density

Abbreviations: 25(OH)D, 25-hydroxyvitamin D; ^{1}H-MRS, monovoxel STEAM magnetic resonance spectroscopy; aLUL, apparent lipid unsaturation level; ANCOVA, analysis of covariance; BMAT, bone marrow adipose tissue; BMD, bone mineral density; BMFF, bone marrow fat fraction; CCI, Charlson comorbidity index; CTX, collagen type 1 cross-linked C-telopeptide; DXA, dual-energy x-ray absorptiometry; MRI, magnetic resonance imaging; PDFF, proton density fat fraction; PINP, procollagen I intact N-terminal; qCT, quantitative computed tomography; ROI, region of interest; TE, echo time; TR, repetition time; UL, olefinic peak; WFI, water-fat separation magnetic resonance imaging.

Osteoporotic fractures are frequent in people older than 50 years: One in 3 women and 1 in 5 men will experience osteoporotic fractures in their lifespan (1, 2). Osteoporosis-related fractures may lead to reduced quality of life, disability, and even death (3-7). Currently, osteoporosis is still underdiagnosed and undertreated (2). Diagnosing osteoporosis and predicting fracture risk depend on case-finding strategies based on the evaluation of bone mineral density (BMD) using dual-energy x-ray absorptiometry (DXA), coupled with an evaluation of clinical risk factors for osteoporosis. However, most fractures arise in people who have not been diagnosed with osteoporosis using BMD screening, or in people who have few clinical risk factors for osteoporosis, or even both (2). Improved methods for identifying individuals with the highest risk of fracture would allow the treatment of patients who would probably have the most favorable benefit-to-risk profiles and may eventually decrease fracture burden.

Noninvasive quantitative assessment of bone marrow adipose tissue (BMAT) using magnetic resonance imaging (MRI) may improve the prediction of fracture (8, 9). Cross-sectional studies have shown that higher BMAT is associated with lower BMD as assessed by DXA and

Received: 5 December 2022. **Editorial Decision:** 31 March 2023. **Corrected and Typeset:** 28 April 2023

quantitative computed tomography (qCT) both in healthy and osteoporotic populations (10-12). Few data are accessible on the relationship between BMAT and osteoporotic fractures (12-16). Previous cross-sectional studies have suggested an association between prevalent vertebral fracture and higher lumbar spine BMAT (12-14). Recently, Woods et al (16) reported an association between higher bone marrow unsaturated lipid content and lower risk of incident vertebral fractures, but not clinical fractures. As such, further investigation is necessary to validate these findings with vertebral fractures, and to evaluate whether BMAT is associated with other osteoporotic fractures. It is important to note that previous studies were not powered to detect meaningful differences between groups. Moreover, these studies were limited by their low numbers of fractures and the inclusion of women and men of all ages, and very few studies have investigated BMAT at the proximal femur (12-14).

Whether noninvasive BMAT measurement can differentiate between individuals with and without osteoporotic fractures still needs to be determined. We conducted this case-control study with the hypothesis that noninvasive BMAT measurement using MRI would be able to differentiate between individuals with and without osteoporotic fractures in postmenopausal women between ages 50 and 90 years. Our main objective was to determine the relationship between lumbar spine BMAT and osteoporotic fractures in postmenopausal women.

Materials and Methods

Study Design

This case-control study (clinicaltrials.gov NCT03219125) included postmenopausal women enrolled by the Department of Rheumatology at Lille University Hospital, France, between October 2018 and June 2021.

For the study, the postmenopausal women were divided into 2 groups: 1 comprising postmenopausal women with recent osteoporotic fractures (< 12 months old, patient cases), and another comprising postmenopausal women with osteoarthritis and no history of fragility fracture (controls).

The study protocol was accepted by the local institutional review board (2017-A00472-51), and the study procedures were in accordance with the ethical standards of the relevant institutional and national human experimentation ethics committees. All patients gave their written informed consent.

Study Population: Patient Cases

Inclusion criteria were (i) postmenopausal women between ages 50 and 90 years, (ii) living in France, and (iii) seen by the Fracture Liaison Service at Lille University Hospital for osteoporotic fractures (eg, a fall from standing height). Osteoporotic fractures were hip, vertebral, proximal humerus, pelvis, ribs, and forearm/wrist fractures (5). To be eligible for the study, patients had to be included and examined within 12 months of diagnosis of the fracture event. Exclusion criteria were (i) implants that are contraindicated for MRI examination, (ii) implants that might pose a health risk or other risks during an MRI, (iii) body mass index (BMI) greater than 38, (iv) weight greater than 140 kg, (v) chronic kidney disease with calculated creatinine clearance less than 30 mL/mn, (vi) diseases known to affect bone metabolism, and (vii) current use of compounds known to affect BMD—including glucocorticoids, osteoporosis medications (bisphosphonates, raloxifene, calcitonin, or teriparatide), and estrogen therapy. Prior use of osteoporosis and estrogen therapy treatments of more than 12 months' duration were allowed.

Study Population: Controls

Inclusion criteria were (i) postmenopausal women between ages 50 and 90 years, (ii) living in France, and (iii) seen by the Department of Rheumatology at Lille University Hospital for osteoarthritis (hips, knees, hands, or spine). Controls were eligible for the study if they reported no previous history of a fragility fracture over age 40 years. Exclusion criteria were the same as those required for cases.

Study Protocol

Information was obtained through a structured interview, a physical examination, biochemical assays, DXA and MRI assessments, and a review of medical records.

Patient disease assessment

Patient characteristics were recorded by 1 physician (J.P., 13 years' experience in osteoporosis management), and a complete physical examination was performed. Osteoporosis risk factors were collected: current smoking, excessive alcohol consumption, previous use of oral corticosteroids (exposed to ≥5 mg/day of prednisolone for ≥3 months), history of fragility fracture over age 40, and hip fracture in mother or father. Data on prior use of estrogen therapy and antiosteoporosis medication over 12 months' duration were also collected. Other data, such as Charlson comorbidity index (CCI), leisure time activity (score 0-15) and medication data, were collected for all participants.

Bone mineral density assessment by dual-energy x-ray absorptiometry

Bone mineral density (BMD) was measured at the lumbar spine (L1-L4) and the nondominant hip by DXA (HOLOGIC Discovery A S/N 81360). The machine was calibrated daily, and quality assurance tests were carried out daily and weekly. World Health Organization criteria were used to define osteoporosis (T score ≤ −2.5) and osteopenia (T score −1.0 to −2.5) based on BMD.

Bone marrow adiposity measurement by magnetic resonance imaging

Image acquisition. All participants underwent an MRI examination on a 3 Tesla system (Ingenia; Philips Healthcare) using the built-in 12-channel posterior body coil and a 16-channel anterior coil. All MRI examinations were performed under the supervision of a senior radiologist (S.B., 11 years' experience). Patients were positioned head first in the supine position. Images were acquired using a conventional protocol—including T1- and T2-weighted, 2-point Dixon turbo-spin echo acquisitions in the sagittal plane—followed by an optional axial T2-weighted, turbo-spin echo acquisition based on the clinical history and the radiologist's observations.

Following this morphological exploration, BMA quantification could be achieved using a 6-echo 3-dimensional gradient-echo sequence (mDixon-Quant; Philips Healthcare), permitting a chemical shift-encoded–based water-fat separation at the lumbar spine (sagittal) and the nondominant proximal femur (coronal oblique). At the lumbar spine, imaging

parameters were repetition time (TR)/echo time (TE)/ΔTE = 11/1.43/1.1 ms; field of view = 220 × 220 mm; voxel size = 1.8 × 1.8 mm; slice thickness = 3 mm; number of excitations = 1; no SENSE acceleration; fold-over direction = foot-head; bandwidth = 1563 Hz; and scan time = 1 minute 41 seconds. At the hip, MR parameters were TR/TE/ΔTE = 11/1.13/1.0 ms; field of view = 354 × 354 mm; voxel size = 1.8 × 1.8 mm; slice thickness = 3 mm; number of excitations = 1; no SENSE acceleration; fold-over direction = right to left; bandwidth = 1724 Hz; and scan time = 1 minute 25 seconds. In both situations, a low flip angle of 3° was used to minimize T1 bias (17).

Offline reconstructions computed proton density fat fraction maps (PDFF; ratio of fat signal over fat and water signals) using a precalibrated 7-peak fat spectrum and a single T2*-correction (18, 19).

Magnetic Resonance Spectroscopy.. To confirm the PDFF measurements obtained from the maps computed from mDixon-Quant acquisitions (full cohort, n = 199), multi-TE monovoxel STEAM MR spectroscopy (^{1}H-MRS) was performed in a subgroup of participants (^{1}H-MRS cohort). ^{1}H-MRS was not completed in the full cohort because of the length of the procedure and technical issues. Therefore, ^{1}H-MRS was performed at the lumbar spine in 131 participants, and at the nondominant proximal femur in 123 participants. The ^{1}H-MRS voxel was positioned in the L3 vertebral body using 3 orthogonal scout sections and T1-weighted acquisitions in the sagittal and axial planes, avoiding the cortical bone. If the L3 vertebral body was fractured, the L2 vertebral body was selected. Similarly, if the nondominant hip was fractured, the ^{1}H-MRS voxel was positioned at the femoral neck of the contralateral hip. ^{1}H-MRS parameters were as follows: volume = 15 × 15 × 15 mm^3; bandwidth = 4000 Hz, with 4096 samples; TR = 2000ms; TE = 10-15-20-25 ms; number of averages = 16; and acquisition time = 3 minutes.

Spectroscopic data were post-processed using the ALFONSO (A versatile Formulation fOr N-dimensional Signal model fitting of MR spectroscopy data) scripts written in MATLAB, version R2022a (MathWorks) (20). The scripts used automatically fitted the acquired spectroscopic data jointly in the time domain, providing reproducible measurements for each acquisition. The fitting strategy used common T2 values and linewidth constraints across all 10 fat peaks (21). PDFF was calculated as the percentage of the fat signal relative to total signal intensity (fat + water). The apparent lipid unsaturation level (aLUL) was calculated as follows, using the olefinic peak (UL) as the most representative unsaturated lipid: aLUL (%) = UL/all fat.

Magnetic resonance segmentation. The MRI acquisitions of each participant were examined by a senior radiologist (S.B., 11 years' experience) on a dedicated workstation, using IntelliSpace Portal (Philips Healthcare) for MR segmentation. First, a morphological assessment was performed to determine the existence of any transitional anomalies, severe degenerative changes, or bone marrow–replacing lesions at the hip or lumbar spine.

Next, the 3 most central slices were chosen at the lumbar spine, based on the PDFF maps computed from the mDixon-Quant acquisitions. A polygonal region of interest (ROI) was drawn in the L1 to L4 vertebral body, avoiding fractured vertebrae, the immediate subchondral bone, bone marrow–replacing lesions, severe degenerative changes, and the basivertebral vein. Fig. 1 shows a PDFF map of the lumbar spine in 2 participants, with the corresponding segmentation. Similarly, an ROI was drawn in the femoral head, femoral neck, and femoral diaphysis based on the 3 most central slices of the coronal oblique mDixon-Quant acquisition of the nondominant hip. Fig. 2 shows a PDFF map of the nondominant hip in 1 participant. The PDFF and aLUL calculated from the postprocessed spectroscopic data reflected fat content and fat composition at the L3 (or L2) level or the femoral neck (Fig. 3).

Repeatability.. To assess the interobserver agreement of the MR analysis, a random subset of 30 participants (15 patients and 15 controls) was selected. Using the same tools and segmentation strategy, PDFF values at the lumbar spine (average of the L1-L4 vertebrae), femoral head, femoral neck, and diaphysis of the nondominant hip were assessed by 2 independents senior radiologists (S.B. and H.K., 11 and 10 years' experience, respectively). For the analysis of the intraobserver agreement, 1 of the 2 senior musculoskeletal radiologists (S.B.) assessed the same subset of participants, with a new segmentation, 3 months later.

Laboratory variables

Fasting blood samples were collected. Total calcium, creatinine, and high-sensitivity C-reactive protein were assessed by routine assays. The estimated glomerular filtration rate was calculated using the Chronic Kidney Disease–Epidemiology Collaboration formula (mL/min). Parathormone was measured by chemiluminescent immunoassay using an automatic analyzer (Architect, Abbott Laboratories). 25-Hydroxyvitamin D (25(OH)D) was measured by competitive chemiluminescent immunoassay using an IDS-iSYS device (IDS). Procollagen I intact N-terminal (PINP) and serum collagen type 1 cross-linked C-telopeptide (CTX) were measured by chemiluminescence assay using the IDS-iSYS Multi-Discipline Automated Analyzer (Immunodiagnostic Systems Inc).

Study Objectives

The primary objective in the full cohort was to compare lumbar spine imaging-based PDFF in patient cases (1a), vertebral fractures (1b), nonvertebral fractures (1c) and controls.

Secondary objectives in the full cohort were to compare hip imaging-based PDFF (femoral head, femoral neck, and femoral diaphysis) in patient cases (2a), vertebral fractures (2b), nonvertebral fractures (2c), and controls.

Secondary objectives in the MRS cohort were to compare L3 MRS-based PDFF in patient cases (3a) and controls—comparison of L3 aLUL in patient cases (3b) and controls; compare femoral neck MRS-based PDFF in patient cases (4a) and controls; and compare femoral neck aLUL in patient cases (4b) and controls.

Study Size

We determined beforehand that we would need to include a total of 194 participants (97 per group) to achieve a statistical power of 80% to demonstrate a mean between-group difference in lumbar spine imaging-based PDFF of 3.5%, as found by Schwartz et al (12). The sample size was calculated based on a 2-sided *t* test with equal variance at a statistical

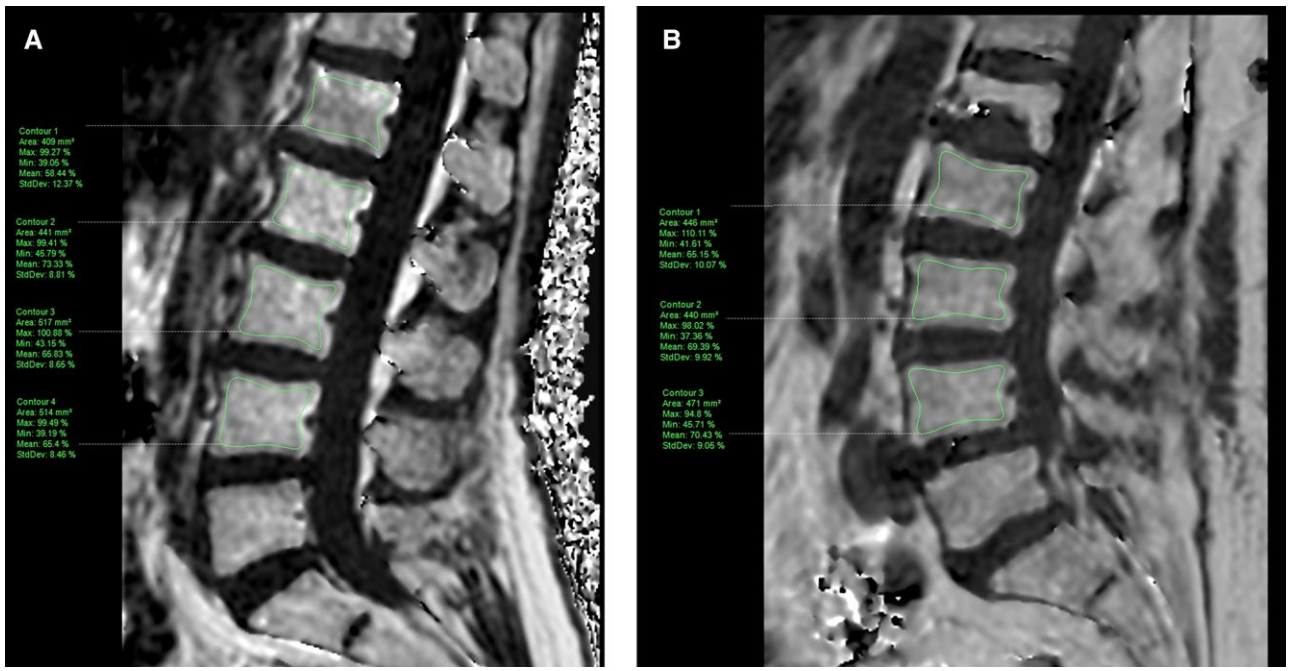

Figure 1. Imaging-based proton density fat fraction (PDFF) map of the lumbar spine. PDFF map of the lumbar spine computed from a T1-weighted, multiecho gradient echo sequence (mDixon-Quant) acquired in the sagittal plane, from an A, 61-year-old control and a B, 90-year-old patient (both postmenopausal women). Manually segmented regions of interest were placed in the L1 to L4 vertebral bodies, avoiding the immediate subchondral bone, the cortical bone and the basivertebral vein. L1 was excluded for patient B, as it was fractured.

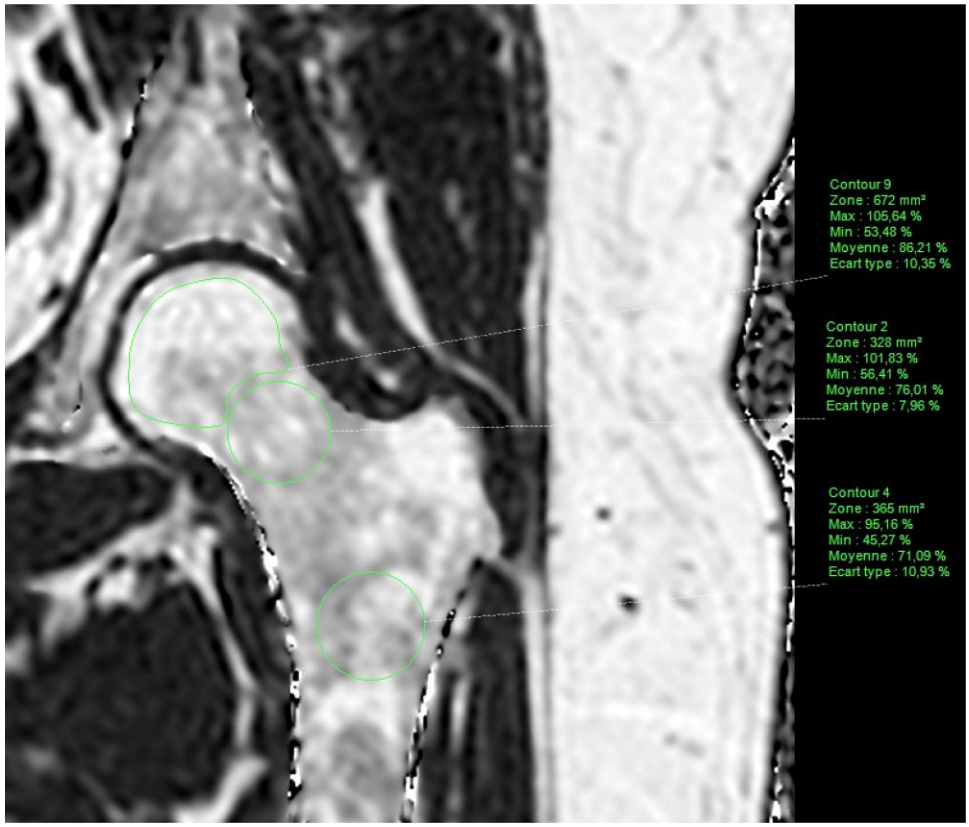

Figure 2. Imaging-based PDFF map of the hip PDFF map of the left (non-dominant) hip computed from a T1-weighted multi-echo gradient echo sequence (mDixon-Quant) acquired in a coronal oblique plane (along the femoral neck axis), from a 55-year old case. Manually segmented ROI was placed in the femoral head, femoral neck, and femoral diaphysis avoiding the cortical bone.

Figure 3. Magnetic resonance spectroscopy (MRS) voxel placement. An MRS (^{1}H-MRS) voxel of interest was placed in the L3 vertebral body (A, T2-weighted sagittal acquisition with fat suppression) and at the femoral neck (B, T1-weighted, gradient echo coronal acquisition) of the nondominant hip. Complementary orthogonal scout acquisitions (not shown) were used to avoid the cortical bone.

significance level of .05, an SD of 8.4% (12), and by considering 5% of missing outcome measures.

Statistical Analysis

Categorical variables are expressed as numbers (percentages). Quantitative variables are expressed as mean (SD) or median (interquartile range) for non-Gaussian distributions. The normality of distributions was assessed using histograms and the Shapiro-Wilk test. In a subset of 30 individuals (15 patient cases and 15 controls), we evaluated the intraobserver and interobserver agreement of imaging-based PDFF measures by calculating the intraclass correlation coefficients with their corresponding 95% CIs. We assessed a selection bias based on the unavailability of ^{1}H-MRS in the full cohort by comparing the patient characteristics of participants with and without ^{1}H-MRS. The magnitude of differences between patient cases and controls was assessed by calculating the effect sizes (standardized differences, calculated on rank-transformed data for non-Gaussian distributions). Absolute values of 0.2, 0.5, and 0.8 in standardized differences were interpreted as a small, medium, and large differences.

In the overall study population, we compared the patient characteristics, biochemistry, BMD, and BMAT measurements of patient cases and controls using the *t* test for quantitative variables (or the Mann-Whitney *U* test for non-Gaussian distributions) and the chi-square test (or Fisher exact test when the expected cell frequency was < 5) for categorical variables, and by calculating effect sizes.

In patient case and control groups separately, we assessed the correlation between imaging-based PDFF measurements and parameters of interest (age, BMD, and PDFF), and the correlation between imaging- and MRS-based PDFF measurements, by calculating the Pearson correlation coefficients, or the Spearman rank correlation coefficients for non-Gaussian distributions, with their 95% CIs. Correlation coefficients (r) in absolute values of 0.1 to 0.3, 0.3 to 0.5, and 0.5 to 1.0 were interpreted as small, medium, and large correlations.

Primary (lumbar spine imaging-based PDFF) and secondary outcome measures (hip imaging- or MRS-based PDFF) in patient cases (overall and according to type of fracture) and controls were compared after adjusting for age, Charlson comorbidity index, and lumbar spine BMD (or hip BMD), using analysis of covariance (ANCOVA). Adjusted means ± SEM and adjusted effect sizes were derived from ANCOVA models.

As a sensitivity analysis, the comparison in outcome measures was performed between patient cases and controls matched by age ±1 year, using optimal matching algorithm without replacement. Comparisons were made using a linear mixed model including matched sets as random effect, and CCI and lumbar spine BMD (or hip BMD) as covariates.

No corrections for multiple testing were made, given the exploratory nature of the study. Secondary outcomes and correlation analyses should be interpreted with caution and as hypothesis generating.

Statistical testing was conducted at the 2-tailed α level of .05. Data were analyzed using SAS software version 9.4 (SAS Institute).

Results

Baseline Characteristics

Table 1 shows the baseline characteristics. In 199 participants (full cohort) with no recent use of bone-active treatment,

Table 1. Patients' general characteristics and biochemistry results at baseline

	No.	Patients (n = 100)	N	Controls (n = 99)	Standardized difference	*P*
Age, y	100	70.2 ± 10.6	99	64.7 ± 8.5	0.56	<.001
Weight, kg	100	67.2 ± 15.6	99	72.1 ± 15.8	−0.33	.027
Height, cm	100	159.1 ± 6.8	99	161.2 ± 6.2	−0.31	.021
BMI	100	26.5 ± 5.9	99	27.7 ± 5.8	−0.21	.14
Leisure time activity (score 0-15)	100	8.7 ± 2.6	99	9.3 ± 2.4	−0.26	.07
Comorbidities						
Nonmetastatic cancer	100	24 (24.0)	99	14 (14.1)	0.25	.08
Type 2 diabetes	100	12 (12.0)	99	12 (12.1)	−0.01	.98
Chronic pulmonary disease	100	9 (9.0)	99	5 (5.1)	0.15	.28
Stroke or TIA	100	9 (9.0)	99	2 (2.0)	0.31	.031
Charlson comorbidity index	100	3 (2-5)	99	2 (0-4)	0.58	<.001
Clinical risk factors						
Excessive alcohol consumption	100	8 (8.0)	99	4 (4.0)	0.17	.24
Current smoking	100	13 (13.0)	99	10 (10.1)	0.09	.52
Family history of hip fracture	100	11 (11.0)	99	11 (11.1)	−0.01	.98
Previous use of corticosteroids	100	6 (6.0)	99	4 (4.0)	0.09	.75
Biochemistry results						
hs-CRP, mg/L	100	3.0 (3.0 to 9.0)	99	3.0 (3.0 to 4.0)	0.33	.021
Calcium, mmol/L	100	2.4 ± 0.1	99	2.4 ± 0.1	0.14	.33
25(OH)D, ng/mL	100	30.1 ± 12.8	99	26.4 ± 9.9	0.32	.025
Serum PTH, pg/mL	100	42.0 (30.0-56.5)	99	47.0 (38.0-59.0)	−0.28	.049
Creatinine, µmol/L	100	62.0 (62.0-71.0)	99	62.0 (53.0-71.0)	0.01	.95
Creatinine clearance (MDRD formula), mL/mn	100	88.0 (77.0-95.5)	99	82.1 (67.1-94.0)	−0.27	.06
PINP, ng/mL	100	72.5 (50.0-99.0)	99	56.0 (40.0-70.0)	0.70	<.001
CTX, pmol/L	100	4058 (2422-5405)	99	2913 (1961-4024)	0.48	<.001
BMD						
BMD lumbar spine, g/cm^2	99[a]	0.847 ± 0.169	99	0.939 ± 0.174	−0.53	<.001
BMD total hip, g/cm^2	97[b]	0.757 ± 0.135	99	0.866 ± 0.145	−0.77	<.001
BMD femoral neck, g/cm^2	97[b]	0.632 ± 0.127	99	0.726 ± 0.122	−0.75	<.001
Fat content (imaging-based)						
PDFF lumbar spine, %	100	59.1 ± 9.6	99	56.6 ± 9.4	0.27	.06
PDFF Femoral head, %	95[c]	90.1 ± 4.0	97[d]	90.0 ± 5.7	0.03	.83
PDFF femoral neck, %	95[c]	82.2 ± 8.1	97[d]	81.5 ± 8.5	0.08	.56
PDFF femoral diaphysis, %	95[c]	81.4 ± 8.5	97[d]	79.8 ± 9.8	0.17	.23

Values expressed as numbers (%), mean ± SD or median (IQR).
Abbreviations: 25(OH)D, 25-hydroxyvitamin D; BMD, bone mineral density; BMI, body mass index; CTX, collagen type 1 cross-linked C-telopeptide; hs-CRP, high-sensitivity C-reactive protein; IQR, interquartile range; MDRD, Modification of Diet in Renal Disease; PDFF, proton density fat fraction; PTH, parathyroid hormone; PINP, procollagen type 1 N-terminal propeptide; TIA, transient ischemic attack.
[a]Lumbar spine BMD measurements were not performed in 1 woman (vertebral fractures at L1, L2, and L3).
[b]Hip BMD measurements were not available in 3 women (bilateral hip arthroplasty).
[c]Hip PDFF measurements were not available in 5 women (bilateral hip arthroplasty, n = 3; unacceptable quality of measurements, n = 2).
[d]Hip PDFF measurements were not performed in 2 women (bilateral hip osteonecrosis, n = 1; unacceptable quality of measurements, n = 1).

controls (n = 99) were significantly younger ($P < .001$), taller ($P = .021$), and heavier ($P = .027$) than patient cases (n = 100). Osteoporosis risk factors in both groups were comparable. CCI was lower in the control group ($P < .001$). Controls had significantly lower 25(OH)D ($P = .025$), PINP, and CTX levels ($P < .001$ for both) than patient cases. We included 52 cases with at least one clinical vertebral fracture (median [minimum-maximum]: 1 [1–4]) and 48 cases with nonvertebral fractures (18 forearm/wrist fractures, 14 hip fractures, 10 pelvis fractures, 5 proximal humerus fractures, and 1 rib fracture). Fifty-nine patient cases had a history of osteoporotic fracture, and 15 had prior osteoporosis treatment (mainly bisphosphonates) that was discontinued more than 12 months before inclusion.

When BMD testing was performed, 43 patient cases were found to have osteoporosis compared to only 11 participants in the control group. Controls had significantly higher BMD at the lumbar spine, femoral neck, and total hip than patient cases ($P < .001$ for all). When imaging based PDFFs were compared, no statistically significant differences between cases and controls were found (see Table 1). Lumbar spine PDFF was higher in patient cases compared to controls, but the difference failed to achieve statistical significance (mean [SD] 59.1% [9.6] vs 56.6% [9.4]; $P = .06$).

Intrareliability and interreliability for lumbar spine imaging-based PDFF measurements were very good, with an intraclass correlation coefficient of 0.98 (95% CI, 0.96-0.99) and 0.94 (95% CI, 0.94-0.97), respectively. Similar findings were found for imaging-based PDFF measurements at the femoral head, neck, and diaphysis (results not shown).

Correlations Between Imaging-based Proton Density Fat Fraction and Parameters of Interest

In both groups, statistically significant positive correlations were found between lumbar spine PDFF and age (patient cases: $R = 0.30$ [0.11-0.47]; $P = .002$; controls: $R = 0.30$ [0.11-0.47]; $P = .002$), suggesting higher lumbar spine PDFF in older women. However, no statistically significant correlations were found between lumbar spine PDFF and BMD measurements, except for total hip BMD (patient cases: $R = -0.21$ [−0.39 to −0.01]; $P = .037$; controls: $R = -0.23$ [−0.4 to −0.03]; $P = .024$), suggesting higher lumbar spine PDFF in women with low total hip BMD.

Table 2 shows the correlations between hip PDFF and parameters of interest. In both groups, statistically significant negative correlations were found between femoral head, neck and diaphysis PDFF and BMD measurements ($P < .05$ for all), except in the control group for the correlation between femoral head PDFF and femoral neck BMD. A statistically significant positive correlation between femoral head, neck, and diaphysis PDFF and age was found only in cases ($R = 0.32$-0.39; $P < .05$ for all). In both groups, femoral head, neck, and diaphysis PDFF were strongly correlated with lumbar spine PDFF ($R = 0.34$-0.49; $P < .001$ for all).

Comparison of Lumbar Spine Imaging-based Proton Density Fat Fraction in Patient Cases and Controls

When lumbar spine PDFFs were compared, after adjusting for age, CCI, and lumbar spine BMD, no statistically significant differences were found between patient cases and controls (adjusted mean [SEM] 58.0% [0.9] vs 57.9% [0.9]; $P = .95$) (1a). When the location of the fractures was considered, no difference in lumbar spine PDFF was found between those with vertebral fractures (1b) or nonvertebral fractures (1c) and controls, even after adjusting for age, CCI, and lumbar spine BMD (Table 3).

Comparison of Hip Imaging-based Proton Density Fat Fraction in Patient Cases and Controls

When femoral head, neck, and diaphysis PDFFs were compared, after adjusting for age and total hip BMD, no statistically significant differences were found between patient cases and controls (2a). Femoral neck PDFF was lower in cases compared to controls, but the difference failed to achieve statistical significance (adjusted mean [SEM] femoral neck PDFF 80.8% [0.8] vs 82.9% [0.8]; $P = .082$) (see Table 3).

In patient cases with vertebral fractures (n = 52), femoral neck PDFF (adjusted mean [SEM] 79.3% [1.2] vs 83.0% [0.8]; $P = .020$) and diaphysis PDFF (adjusted mean [SEM] 77.7% [1.4] vs 81.6% [0.9]; $P = .029$) were found to be lower than in controls (n = 99) (2b) (see Table 3). No difference in hip PDFF (femoral head, femoral neck, and femoral diaphysis) was found between patient cases with nonvertebral fractures (n = 42) and the control group (n = 99) (2c).

A sensitivity analysis on age-matched sets (± 1 year) was performed and found similar effect size estimates (Supplementary Table S1) (22).

Magnetic Resonance Spectroscopy-based Proton Density Fat Fraction and Apparent Lipid Unsaturation Level at the L3 Vertebral Level and Femoral Neck

^{1}H-MRS was performed at the L3 vertebral level in a subgroup of 131 participants. No statistically significant differences in demographic, fractures, and clinical characteristics were found between the 131 participants (^{1}H-MRS cohort) and the 68 noncompleters. As illustrated in Table 4, no statistically significant differences in PDFF (3a) or aLUL (3b) at the L3 level were found between groups.

At the femoral neck, after adjustment on age, CCI, and femoral neck BMD, femoral neck PDFF (4a), but not aLUL (4b), was found to be lower in cases than in controls (adjusted mean [SEM] 78.3% [1.3] vs 82.3% [1.1]; $P = .028$) (see Table 4).

In both groups, femoral neck MRS-based PDFF was highly correlated with femoral neck imaging-based PDFF measurements (patient cases: $R = 0.89$ [0.81-0.93]; $P < .0001$; controls: $R = 0.88$ [0.81-0.93]; $P < .0001$). Similar findings were found for L3 MRS-based PDFF and lumbar spine imaging-based PDFF (patient cases: $R = 0.77$ [0.62-0.86]; $P < .0001$; controls: $R = 0.84$ [0.74-0.90]; $P < .0001$).

Discussion

When lumbar spine imaging-based PDFF in patient cases (overall and according to type of fracture) and controls were compared, no statistically significant differences were found. Another finding is that lower femoral neck and femoral diaphysis PDFF derived from water-fat imaging was associated with clinical vertebral fractures in postmenopausal women, independently of age, CCI, and BMD. This result suggests that PDFF measurements at the proximal femur, rather than at the lumbar spine, may be useful in assessing fracture risk in this population. ^{1}H-MRS measurements were strongly correlated with imaging-based PDFF values and confirmed the association between PDFF and osteoporotic fractures at the femoral neck, while also supporting the use of chemical shift-encoded–based water-fat separation imaging to explore BMAT.

Lumbar Spine Bone Marrow Adipose Tissue and Clinical Fractures

There are few studies on the association between BMAT and clinical fractures. Most of the studies addressing this question were limited by a small number of participants with a prevalent clinical fracture. Schwartz et al (12) failed to find an association between lumbar spine bone marrow fat fraction (BMFF) measured using ^{1}H-MRS and history of clinical fractures (all fractures), or analyses limited to fragility fractures (clinical spine, proximal humerus, and hip), whether in women or men. Findings in accordance with these results have been published by Patsch et al (14). In that study, the authors found no association between fragility fractures (in 36 patients, mostly nonvertebral fractures) and lumbar spine BMFF measured using ^{1}H-MRS (14). In accordance with the results of previous ^{1}H-MRS studies (12, 14), we did not find an association between lumbar spine PDFF and osteoporotic fractures in the ^{1}H-MRS cohort or in the full imaging-based cohort.

Table 2. Correlations between hip imaging-based proton density fat fraction and parameters of interest

	Patients (n = 100)			Controls (n = 99)		
	Femoral head PDFF, %[a]	Femoral neck PDFF, %[a]	Femoral diaphysis PDFF, %[a]	Femoral head PDFF, %[b]	Femoral neck PDFF, %[b]	Femoral diaphysis PDFF, %[b]
Age, y	R = 0.32 (0.13 to 0.49) *P* = .001	R = 0.37 (0.19 to 0.53) *P* < .001	R = 0.39 (0.2 to 0.55) *P* < .0001	R = 0.12 (−0.08 to 0.31) *P* = .23	R = 0.08 (−0.12 to 0.28) *P* = .43	R = 0.13 (−0.07 to 0.32) *P* = .20
Lumbar spine BMD, g/cm^{2}[c]	R = −0.35 (−0.52 to −0.16) *P* < .001	R = −0.28 (−0.45 to −0.08) *P* = .006	R = −0.26 (−0.44 to −0.07) *P* = .009	R = −0.25 (−0.43 to −0.05) *P* = .014	R = −0.41 (−0.56 to −0.23) *P* < .0001	R = −0.39 (−0.54 to −0.2) *P* < .0001
Femoral neck BMD, g/cm^{2}[d]	R = −0.25 (−0.43 to −0.05) *P* = .013	R = −0.21 (−0.4 to −0.01) *P* = .038	R = −0.27 (−0.45 to −0.07) *P* = .008	R = −0.16 (−0.34 to 0.05) *P* = .13	R = −0.29 (−0.46 to −0.1) *P* = .004	R = −0.29 (−0.46 to −0.09) *P* = .004
Total hip BMD, g/cm^{2}[d]	R = −0.32 (−0.49 to −0.12) *P* = .002	R = −0.29 (−0.46 to −0.09) *P* = .004	R = −0.38 (−0.54 to −0.2) *P* = .0001	R = −0.29 (−0.46 to −0.09) *P* = .004	R = −0.46 (−0.61 to −0.29) *P* < .0001	R = −0.46 (−0.6 to −0.29) *P* < .0001
Lumbar spine PDFF, %	R = 0.38 (0.19 to 0.54) *P* = .0001	R = 0.49 (0.31 to 0.63) *P* < .0001	R = 0.49 (0.31 to 0.63) *P* < .0001	R = 0.34 (0.15 to 0.51) *P* < .001	R = 0.39 (0.2 to 0.54) *P* < .0001	R = 0.48 (0.31 to 0.62) *P* < .0001

Abbreviations: BMD, bone mineral density; PDFF, proton density fat fraction (imaging-based).
[a]n = 95; Hip PDFF measurements were not available in 5 women (bilateral hip arthroplasty, n = 3; unacceptable quality of measurements, n = 2).
[b]n = 97; Hip PDFF measurements were not performed in 2 women (bilateral hip osteonecrosis, n = 1; unacceptable quality of measurements, n = 1).
[c]n = 198; Lumbar spine BMD measurements were not performed in 1 woman (vertebral fractures at L1, L2, and L3).
[d]n = 196; Hip BMD measurements were not available in 3 women (bilateral hip arthroplasty).

Table 3. Adjusted mean imaging-based proton density fat fraction was assessed by presence of fracture vs no fracture

	No.	Patients	No.	Controls	Standardized difference	*P*
All fractures (n = 100)						
PDFF lumbar spine, %	100	58.0 ± 0.9	99	57.9 ± 0.9	0.01 (−0.25 to 0.27)	.95
PDFF femoral head, %	95[a]	89.5 ± 0.5	97[b]	90.6 ± 0.5	−0.21 (−0.47 to 0.06)	.125
PDFF femoral neck, %	95[a]	80.8 ± 0.8	97[b]	82.9 ± 0.8	−0.23 (−0.48 to 0.03)	.082
PDFF femoral diaphysis, %	95[a]	79.6 ± 0.9	97[b]	81.5 ± 0.9	−0.19 (−0.44 to 0.06)	.140
Vertebral fractures (n = 52)						
PDFF lumbar spine, %	52	57.4 ± 1.4	99	58.0 ± 1.0	−0.06 (−0.37 to 0.25)	.71
PDFF femoral head, %	48[c]	89.1 ± 0.8	97[b]	90.6 ± 0.5	−0.25 (−0.57 to 0.08)	.134
PDFF femoral neck, %	48[c]	79.3 ± 1.2	97[b]	83.0 ± 0.8	−0.37 (−0.69 to −0.06)	.020
PDFF femoral diaphysis, %	48[c]	77.7 ± 1.4	97[b]	81.6 ± 0.9	−0.34 (−0.65 to −0.04)	.029
Nonvertebral fractures (n = 48)						
PDFF lumbar spine, %	48	57.3 ± 1.3	99	57.0 ± 0.9	0.03 (−0.29 to 0.35)	.83
PDFF femoral head, %	47[d]	89.2 ± 0.7	97[b]	90.3 ± 0.5	−0.20 (−0.52 to 0.13)	.24
PDFF femoral neck, %	47[d]	80.8 ± 1.1	97[b]	82.2 ± 0.8	−0.15 (−0.47 to 0.16)	.34
PDFF femoral diaphysis, %	47[d]	79.6 ± 1.2	97[b]	80.7 ± 0.8	−0.10 (−0.41 to 0.20)	.52

Primary (lumbar spine imaging-based PDFF) and secondary outcome measures (hip imaging-based PDFF) in cases (overall and according to the type of fracture) and controls were compared, after adjusting for age, Charlson comorbidity index, and lumbar spine BMD (or hip BMD), using analysis of covariance (ANCOVA). Adjusted means ± SEM and adjusted effect sizes were derived from ANCOVA models.
Abbreviations: BMD, bone mineral density; PDFF, proton density fat fraction.
[a]Hip PDFF measurements were not available in 5 women (bilateral hip arthroplasty, n = 3; unacceptable quality of measurements, n = 2).
[b]Hip PDFF measurements were not performed in 2 women (bilateral hip osteonecrosis, n = 1; unacceptable quality of measurements, n = 1).
[c]Hip PDFF measurements were not available in 4 women (bilateral hip arthroplasty, n = 2; unacceptable quality of measurements, n = 2).
[d]Hip PDFF measurements were not available in 1 woman (bilateral hip arthroplasty, n = 1).

Table 4. Comparison of proton density fat fraction and apparent lipid unsaturation level using magnetic resonance imaging with spectroscopy in patients and controls

	No.	Patients N = 60[a]	No.	Controls N = 71	Standardized difference	*P*
L3 PDFF, %	53[b]	57.4 (1.5)	60[c]	57.4 (1.4)	−0.004 (−0.36 to 0.35)	.98
L3 aLUL, %	53[b]	4.2 (0.08)	60[c]	4.2 (0.07)	0.05 (−0.31 to 0.41)	.79
	No.	**Patients N = 54**	**No.**	**Controls N = 69**	**Standardized difference**	***P***
Femoral neck PDFF, %	51[d]	78.3 (1.3)	65[e]	82.3 (1.1)	−0.38 (−0.71 to −0.04)	.028
Femoral neck aLUL, %	51[d]	3.7 (0.09)	65[e]	3.6 (0.08)	0.08 (−0.27 to 0.42)	.66

Results are shown as adjusted mean ± SEM calculated from the least square means of the analysis of covariance model adjusted for age, Charlson comorbidity index, and BMD (lumbar spine or femoral neck).
Abbreviations: aLUL, apparent lipid unsaturation level; BMD, bone mineral density; PDFF, proton density fat fraction.
[a]There were 29 vertebral fractures and 31 nonvertebral fractures.
[b]Lumbar spine measurements were not available in 7 patients (poor acquisition quality, n = 2; poor fitting, n = 5).
[c]Lumbar spine measurements were not available in 11 controls (poor acquisition quality, n = 7; poor fitting, n = 4).
[d]Hip measurements were not available in 3 patients (poor acquisition quality, n = 1; poor fitting, n = 2).
[e]Hip measurements were not available in 4 controls (poor acquisition quality, n = 2; poor fitting, n = 2).

However, femoral neck PDFF was lower in postmenopausal women with recent osteoporotic fractures. This result was observed only in the ^{1}H-MRS cohort, but not in the full imaging-based cohort either at the lumbar spine or proximal femur. To the best of our knowledge, no previous studies of BMAT and fractures in older participants have used ^{1}H-MRS or WFI to measure proximal femur PDFF.

Lumbar Spine Bone Marrow Adipose Tissue and Vertebral Fractures

Some preliminary human imaging studies have suggested that changes in lumbar spine BMFF, assessed using ^{1}H-MRS, may contribute to "vertebral bone weakness," independently of BD (23, 24). Sometime later, Schwartz and colleagues (12) reported an association between prevalent vertebral fractures and higher lumbar spine BMFF measured by ^{1}H-MRS in older men (n = 118) but not in women (n = 139). More recently, Gassert et al (15) demonstrated that lumbar spine PDFF measured using WFI has the potential to discriminate between patients with and without recent vertebral (osteoporotic and nonosteoporotic) fractures. Unlike previous studies, we found no association between lumbar spine PDFF and clinical vertebral fractures, using either imaging- or MRS-based measurements.

However, we found that lower femoral neck and diaphysis imaging-based PDFF was associated with vertebral fractures, which is a novel and unexpected finding.

Fat Composition and Fractures

In a study including 50 postmenopausal women (mean age: 70 years; 15 with normal BMD, 15 with osteopenia, 20 with osteoporosis) and 12 young women as controls (mean age: 28 years), Yeung et al (11) observed that the fat unsaturation index was significantly lower in osteoporotic and osteopenic individuals compared to normal participants and young controls. In another study using lumbar spine ^{1}H-MRS involving 69 diabetic and nondiabetic postmenopausal women, the prevalence of fragility fractures was significantly associated with lower unsaturation levels, independently of age, race, and lumbar spine volumetric BMD (14). However, Woods et al (16) failed to find any association between unsaturated lipid levels (measured at the lumbar spine using ^{1}H-MRS) and prevalent vertebral fractures in 465 participants from the Age Gene/Environment Susceptibility (AGES)-Reykjavik study . Unlike Patsch et al (14), we did not find an association between aLUL and clinical fractures at L3 or femoral neck.

Longitudinal Studies

In the AGES-Reykjavik study, there were no associations between BMFF, incident radiographic vertebral fractures, and incident clinical fractures in women or men (25). However, the authors recently found an association between higher levels of unsaturated marrow lipid and a lower risk of incident radiographic vertebral fractures and, in men, but not women, a lower risk of incident clinical fractures (16). Future longitudinal studies of BMAT and BD and fracture outcomes are necessary and reported measurements of BMFF and lipid unsaturation levels at the proximal femur are needed.

Possible Mechanisms

Why we failed to find associations between lumbar spine PDFF and osteoporotic fractures is unclear. Although severe degenerative changes were considered when measuring lumbar spine PDFF, osteoarthritis and osteoporosis might lead to an increase in PDFF by sharing common pathophysiological pathways. Differences between osteoporosis and osteoporosis + osteoarthritis might have been attenuated by not considering osteoarthritis (26). The same uncertainty remains regarding the association between lower femoral neck and diaphysis PDFF and vertebral fractures, especially since several studies have reported an association between prevalent vertebral fractures and higher lumbar spine BMAT. Of course, the relationship between bone and fat is complex, since the associations between adiposity and bone are age-, sex-, menopausal status-, bone compartment-, and adipose depot–specific (8, 27). In line with this, we believe that the association between BMAT and fractures is also complex, differs across skeletal sites, and is modified by the interaction between BMAT, age, and BMD. Moreover, future studies investigating BMAT and bone health in older individuals should assess skeletal muscle mass and function in the continuous interface and communication with each other (bone, fat, and muscle).

Strengths and Limitations

This study has several strengths: (1) To the best of our knowledge, it is the first that was powered to detect meaningful differences between groups, and to include participants with recent fractures with a balanced number of vertebral and nonvertebral fractures; (2) our study population is homogeneous, comprising exclusively postmenopausal women to prevent heterogeneity due to sex and menopausal status; (3) BMAT was measured both at the lumbar spine and the proximal femur with 2 different MRI techniques that have been previously demonstrated as roughly equivalent (28); (4) we chose DXA —the clinical standard for BMD measurements—over qCT. Indeed, qCT is not used for routine clinical diagnostic workup in osteoporotic patients; and (5) MRI and DXA images were all acquired on the same machines.

This study also has several limitations. The cross-sectional design prevented us from assessing the temporal association between PDFF and BD and fracture outcomes. Another limitation of this study is the lack of age matching. However, the regression models were adjusted for this parameter, which does not modify our findings. The study sample size was based on an estimation of difference in lumbar spine imaging-based PDFF between patient cases and controls. Therefore, the study is not adequately powered for comparison between specific fracture types (vertebral fractures and nonvertebral fractures) with controls, and hence the findings reported on femoral neck/diaphysis PDFF in relation to vertebral fractures are only indicative and may be due to chance or small sample bias. Another limitation is the choice of women with osteoarthritis as the control group. In addition, these results are limited to postmenopausal women and do not apply to men and younger age groups.

Conclusions

No difference in lumbar spine PDFF was found between those with osteoporotic fractures and controls. However, proximal femur imaging-based PDFF might be a noninvasive biomarker that can differentiate between postmenopausal women with and without vertebral fractures. As such, as a complement to BMD, PDFF may be a useful radiation-free tool for assessing bone fragility. Whether proximal femur PDFF improves the identification of postmenopausal women at risk of osteoporotic fractures requires validation in prospective studies. We recommend that future studies investigating BMAT and bone health report measurements of proximal femur PDFF rather than lumbar spine PDFF alone. Finally, the recent Bone Marrow Adiposity Society methodological recommendations should be used (29). The aim is to standardize imaging protocols and increase comparability across studies and sites.

Acknowledgments

These analyses were presented in part as an oral presentation at the Bone Marrow Adiposity Society meeting; September 30, 2022, Athens, Greece.

Funding

This work was supported by an unrestricted grant from MSDAVENIR France.

Author Contributions

J.P.: conceptualization, methodology, project administration, visualization, writing—original draft; S.B.: data curation, formal analysis, writing—review, and editing; D.L.: formal analysis, methodology, validation, writing—review, and editing; H.K.: formal analysis, validation, writing—review, and editing; V.D.: formal analysis, methodology,

validation, writing—review, and editing; S.R.: supervision, validation, writing—review, and editing; D.C.K.: supervision, validation, writing—review, and editing; A.C.: supervision, validation, writing—review, and editing; and B.C.: conceptualization, funding acquisition, methodology, supervision, validation, writing—review, and editing.

Disclosures

J.P. has received honoraria from Amgen, MSD, Eli Lilly, and Pfizer. B.C. has received honoraria from Amgen, Eli Lilly, Expanscience, Ferring, Medtronic, Novartis, Nordic, Roche Diagnostics, and Theramex. The remaining authors have nothing to disclose.

Data Availability

The data that support the findings of this study are available from the corresponding author on reasonable request.

References

1. NIH Consensus Development Panel on Osteoporosis Prevention, Diagnosis, and Therapy. Osteoporosis prevention, diagnosis, and therapy. *JAMA*. 2001;285(6):785-795.
2. Borgström F, Karlsson L, Ortsäter G, *et al*; International Osteoporosis Foundation. Fragility fractures in Europe: burden, management and opportunities. *Arch Osteoporos*. 2020;15(1):59.
3. Klotzbuecher CM, Ross PD, Landsman PB, Abbott TA III, Berger M. Patients with prior fractures have an increased risk of future fractures: a summary of the literature and statistical synthesis. *J Bone Miner Res*. 2010;15(4):721-739.
4. van Geel TACM, van Helden S, Geusens PP, Winkens B, Dinant GJ. Clinical subsequent fractures cluster in time after first fractures. *Ann Rheum Dis*. 2009;68(1):99-102.
5. Bliuc D, Nguyen ND, Milch VE, Nguyen TV, Eisman JA, Center JR. Mortality risk associated with low-trauma osteoporotic fracture and subsequent fracture in men and women. *JAMA*. 2009;301(5):513-521.
6. Cooper C. The crippling consequences of fractures and their impact on quality of life. *Am J Med*. 1997;103(2A):S12-S19.
7. Haleem S, Lutchman L, Mayahi R, Grice JE, Parker MJ. Mortality following hip fracture: trends and geographical variations over the last 40 years. *Injury*. 2008;39(10):1157-1163.
8. Paccou J, Penel G, Chauveau C, Cortet B, Hardouin P. Marrow adiposity and bone: review of clinical implications. *Bone*. 2019;118:8-15.
9. Paccou J, Hardouin P, Cotten A, Penel G, Cortet B. The role of bone marrow fat in skeletal health: usefulness and perspectives for clinicians. *J Clin Endocrinol Metab*. 2015;100(10):3613-3621.
10. Shen W, Chen J, Punyanitya M, Shapses S, Heshka S, Heymsfield SB. MRI-measured bone marrow adipose tissue is inversely related to DXA-measured bone mineral in Caucasian women. *Osteoporos Int*. 2007;18(5):641-647.
11. Yeung DKW, Griffith JF, Antonio GE, Lee FKH, Woo J, Leung PC. Osteoporosis is associated with increased marrow fat content and decreased marrow fat unsaturation: a proton MR spectroscopy study. *J Magn Reson Imaging*. 2005;22(2):279-285.
12. Schwartz AV, Sigurdsson S, Hue TF, *et al*. Vertebral bone marrow fat associated with lower trabecular BMD and prevalent vertebral fracture in older adults. *J Clin Endocrinol Metab*. 2013;98(6):2294-2300.
13. Wehrli FW, Hopkins JA, Hwang SN, Song HK, Snyder PJ, Haddad JG. Cross-sectional study of osteopenia with quantitative MR imaging and bone densitometry. *Radiology*. 2000;217(2):527-538.
14. Patsch JM, Li X, Baum T, *et al*. Bone marrow fat composition as a novel imaging biomarker in postmenopausal women with prevalent fragility fractures. *J Bone Miner Res*. 2013;28(8):1721-1728.
15. Gassert FT, Kufner A, Gassert FG, *et al*. MR-based proton density fat fraction (PDFF) of the vertebral bone marrow differentiates between patients with and without osteoporotic vertebral fractures. *Osteoporos Int*. 2022;33(2):487-496.
16. Woods G, Ewing S, Schafer A, *et al*. Saturated and unsaturated bone marrow lipids have distinct effects on bone density and fracture risk in older adults. *J Bone Miner Res*. 2022;37(4):700-710.
17. Karampinos DC, Yu H, Shimakawa A, Link TM, Majumdar S. T_1-corrected fat quantification using chemical shift-based water/fat separation: application to skeletal muscle. *Magn Reson Med*. 2011;66(5):1312-1326.
18. Ren J, Dimitrov I, Sherry AD, Malloy CR. Composition of adipose tissue and marrow fat in humans by ^{1}H NMR at 7 Tesla. *J Lipid Res*. 2008;49(9):2055-2062.
19. Karampinos DC, Ruschke S, Dieckmeyer M, *et al*. Quantitative MRI and spectroscopy of bone marrow. *J Magn Reson Imaging*. 2018;47(2):332-353.
20. Ruschke S, Karampinos DC. ALFONSO: A versatiLe formulation fOr N-dimensional signal mOdel fitting of MR spectroscopy data and its application in MRS of body lipids. Proceedings of the 31st Joint Annual Meeting of the International Society for Magnetic Resonance in Medicine and the European Society for Magnetic Resonance in Medicine and Biology; 2022:2776.
21. Hamilton G, Yokoo T, Bydder M, *et al*. In vivo characterization of the liver fat ^{1}H MR spectrum. *NMR Biomed*. 2011;24(7):784-790.
22. Paccou J, Badr S, Lombardo D, *et al*. Supplementary data for "Bone marrow adiposity and fragility fractures in postmenopausal women: the ADIMOS case-control study." Generic Digital Repository. 2023.
23. Schellinger D, Lin CS, Lim J, Hatipoglu HG, Pezzullo JC, Singer AJ. Bone marrow fat and bone mineral density on proton MR spectroscopy and dual-energy X-ray absorptiometry: their ratio as a new indicator of bone weakening. *AJR Am J Roentgenol*. 2004;183(6):1761-1765.
24. Schellinger D, Lin CS, Hatipoglu HG, Fertikh D. Potential value of vertebral proton MR spectroscopy in determining bone weakness. *AJNR Am J Neuroradiol*. 2001;22(8):1620-1627.
25. Woods GN, Ewing SK, Sigurdsson S, *et al*. Greater bone marrow adiposity predicts bone loss in older women. *J Bone Miner Res*. 2020;35(2):326-332.
26. Li G, Xu Z, Fan J, *et al*. To assess differential features of marrow adiposity between postmenopausal women with osteoarthritis and osteoporosis using water/fat MRI. *Menopause*. 2017;24(1):105-111.
27. Devlin MJ, Rosen CJ. The bone-fat interface: basic and clinical implications of marrow adiposity. *Lancet Diabetes Endocrinol*. 2015;3(2):141-147.
28. Karampinos DC, Melkus G, Baum T, Bauer JS, Rummeny EJ, Krug R. Bone marrow fat quantification in the presence of trabecular bone: initial comparison between water-fat imaging and single-voxel MRS. *Magn Reson Med*. 2014;71(3):1158-1165.
29. Tratwal J, Labella R, Bravenboer N, *et al*. Reporting guidelines, review of methodological standards, and challenges toward harmonization in bone marrow adiposity research. Report of the Methodologies Working Group of the International Bone Marrow Adiposity Society. *Front Endocrinol (Lausanne)*. 2020;11:65.